# REPORT DOCUMENTATION PAGE

Form Approved OMB NO. 0704-0188



| 1. REPORT DATE (DD-MM-YYYY) | 2. REPORT TYPE | 3. DATES COVERED (From - To) |
|---|---|---|
| 04-09-2015 | Final Report | 18-Aug-2014 - 17-May-2015 |

**4. TITLE AND SUBTITLE**
Final Report: Scalable Directed Self-Assembly Using Ultrasound Waves

**5a. CONTRACT NUMBER**
W911NF-14-1-0565

**5b. GRANT NUMBER**

**5c. PROGRAM ELEMENT NUMBER**
611102

**6. AUTHORS**
Bart Raeymaekers

**5d. PROJECT NUMBER**

**5e. TASK NUMBER**

**5f. WORK UNIT NUMBER**

**7. PERFORMING ORGANIZATION NAMES AND ADDRESSES**
University of Utah
75 South 2000 East

Salt Lake City, UT 84112 -8930

**8. PERFORMING ORGANIZATION REPORT NUMBER**

**9. SPONSORING/MONITORING AGENCY NAME(S) AND ADDRESS (ES)**
U.S. Army Research Office
P.O. Box 12211
Research Triangle Park, NC 27709-2211

**10. SPONSOR/MONITOR'S ACRONYM(S)**
ARO

**11. SPONSOR/MONITOR'S REPORT NUMBER(S)**
65819-MS-II.2

**12. DISTRIBUTION AVAILIBILITY STATEMENT**
Approved for Public Release; Distribution Unlimited

**13. SUPPLEMENTARY NOTES**
The views, opinions and/or findings contained in this report are those of the author(s) and should not contrued as an official Department of the Army position, policy or decision, unless so designated by other documentation.

**14. ABSTRACT**
We aim to understand how ultrasound waves can be used to create organized patterns of nanoparticles in a host medium such as a polymer matrix material. The critical difference between the ultrasound technology studied in this project, and other directed self-assembly techniques is its scalability and flexibility. During this 9 month project, we have derived the theory and implemented a model to simulate how patterns of nanoparticles dispersed in a host medium are assembled by means of standing ultrasound waves. Additionally, we have obtained experimental validation of this model. This research finds application in design and processing of novel bulk

**15. SUBJECT TERMS**
directed self-assembly, nanoparticles, multi-functional materials, bulk processing

| 16. SECURITY CLASSIFICATION OF: | | | 17. LIMITATION OF ABSTRACT | 15. NUMBER OF PAGES | 19a. NAME OF RESPONSIBLE PERSON |
|---|---|---|---|---|---|
| a. REPORT | b. ABSTRACT | c. THIS PAGE | | | Bart Raeymaekers |
| UU | UU | UU | UU | | 19b. TELEPHONE NUMBER: 801-585-7594 |

**Report Title**

Final Report: Scalable Directed Self-Assembly Using Ultrasound Waves


**ABSTRACT**

We aim to understand how ultrasound waves can be used to create organized patterns of nanoparticles in a host medium such as a polymer matrix material. The critical difference between the ultrasound technology studied in this project, and other directed self-assembly techniques is its scalability and flexibility. During this 9 month project, we have derived the theory and implemented a model to simulate how patterns of nanoparticles dispersed in a host medium are assembled by means of standing ultrasound waves. Additionally, we have obtained experimental validation of this model. This research finds application in design and processing of novel bulk materials and could lead to processing of bulk nanocomposite materials with tailored properties.


---

## Enter List of papers submitted or published that acknowledge ARO support from the start of the project to the date of this printing. List the papers, including journal references, in the following categories:

### (a) Papers published in peer-reviewed journals (N/A for none)

| Received | | Paper |
|---|---|---|
| 09/03/2015 | 1.00 | Mathieu Francoeur, Bart Raeymaekers, Shandra J. Corbitt. Implementation of optical dielectric metamaterials: A review, Journal of Quantitative Spectroscopy and Radiative Transfer, (06 2015): 3. doi: 10.1016/j.jqsrt.2014.12.009 |
| **TOTAL:** | **1** | |

**Number of Papers published in peer-reviewed journals:**

---

### (b) Papers published in non-peer-reviewed journals (N/A for none)

| Received | | Paper |
|---|---|---|
| **TOTAL:** | | |

**Number of Papers published in non peer-reviewed journals:**

---

### (c) Presentations

**Number of Presentations:** 0.00

## Non Peer-Reviewed Conference Proceeding publications (other than abstracts):

Received Paper

**TOTAL:**

**Number of Non Peer-Reviewed Conference Proceeding publications (other than abstracts):**

## Peer-Reviewed Conference Proceeding publications (other than abstracts):

Received Paper

**TOTAL:**

**Number of Peer-Reviewed Conference Proceeding publications (other than abstracts):**

## (d) Manuscripts

Received Paper

**TOTAL:**

**Number of Manuscripts:**

## Books

Received Book

**TOTAL:**

| Received | Book Chapter |
|---|---|

**TOTAL:**

## Patents Submitted

## Patents Awarded

## Awards

John Greenhall, the main PhD student funded by this contract, obtained the 2015 National Aeronautics and Space Agency (NASA) NSTRF fellowship, awarded by the NASA Office of the Chief Technologist.

## Graduate Students

| NAME | PERCENT_SUPPORTED | Discipline |
|---|---|---|
| John Greenhall | 1.00 | |
| Michael Price | 0.33 | |
| Leora Homel | 0.01 | |
| **FTE Equivalent:** | **1.34** | |
| **Total Number:** | **3** | |

## Names of Post Doctorates

| NAME | PERCENT_SUPPORTED |
|---|---|
| **FTE Equivalent:** | |
| **Total Number:** | |

## Names of Faculty Supported

| NAME | PERCENT_SUPPORTED | National Academy Member |
|---|---|---|
| Bart Raeymaekers | 0.15 | No |
| **FTE Equivalent:** | **0.15** | |
| **Total Number:** | **1** | |

## Names of Under Graduate students supported

| NAME | PERCENT_SUPPORTED | Discipline |
|---|---|---|
| Jacob Bryan | 0.01 | Mechanical Engineering |
| **FTE Equivalent:** | **0.01** | |
| **Total Number:** | **1** | |

## Student Metrics

This section only applies to graduating undergraduates supported by this agreement in this reporting period

The number of undergraduates funded by this agreement who graduated during this period: ..... 0.00

The number of undergraduates funded by this agreement who graduated during this period with a degree in science, mathematics, engineering, or technology fields:..... 0.00

The number of undergraduates funded by your agreement who graduated during this period and will continue to pursue a graduate or Ph.D. degree in science, mathematics, engineering, or technology fields:..... 0.00

Number of graduating undergraduates who achieved a 3.5 GPA to 4.0 (4.0 max scale):..... 0.00

Number of graduating undergraduates funded by a DoD funded Center of Excellence grant for Education, Research and Engineering:..... 0.00

The number of undergraduates funded by your agreement who graduated during this period and intend to work for the Department of Defense ..... 0.00

The number of undergraduates funded by your agreement who graduated during this period and will receive scholarships or fellowships for further studies in science, mathematics, engineering or technology fields: ..... 0.00

## Names of Personnel receiving masters degrees

NAME

**Total Number:**

## Names of personnel receiving PHDs

NAME

**Total Number:**

## Names of other research staff

NAME PERCENT_SUPPORTED

**FTE Equivalent:**
**Total Number:**

## Sub Contractors (DD882)

## Inventions (DD882)

## Scientific Progress

See attachment

## Technology Transfer

LJ Holmes: I have visited LJ Holmes's research group (Micro-Compositronics and Rapid Operations Lab) in July 2013 at Aberdeen Proving Grounds (APG), to discuss a possible collaboration. The idea is to integrate the ultrasound directed self-assembly technique with additive manufacturing. LJ is an expert in additive manufacturing and showed me around his laboratory and several other labs at APG, I also gave a seminar at APG during that visit. During the STIR grant, I have kept regular contact with LJ and have solicited his feedback to ensure that our research is in line with the Army mission.

Steve Taulbee: Steve Taulbee visited the University of Utah in January 2015 and I briefly met with him to discuss the Army Research on which we are working. Steve invited me to visit APG again, and I have given a seminar at APG in April 2015, in addition to meeting again with LJ Holmes, Ray Brennan, and others, to discuss our research progress in light of Army needs and future directions.

Raymond Brennan: I have had several phone conversations about the fit and a possible collaboration with the Energy Coupled to Matter program, with Ray Brennan. We plan to extend the research performed during this STIR contract to use ultrasound directed self-assembly for manufacturing of multi-functional materials, and we will collaborate with Ray on this effort.

**Table of contents**



List of Appendices

# Final report: Scalable directed self-assembly using ultrasound waves

Army Research Office STIR contract W911NF1410565
Bart Raeymaekers, Assistant Professor
Department of Mechanical Engineering - University of Utah

**Synopsis**

We aim to understand how ultrasound waves can be used to create organized patterns of nanoparticles in a host medium such as a polymer matrix material. The critical difference between the ultrasound technology studied in this project, and other directed self-assembly techniques is its scalability and flexibility. During this 9 month project, we have derived the theory and implemented a model to simulate how patterns of nanoparticles dispersed in a host medium are assembled by means of standing ultrasound waves. Additionally, we have obtained experimental validation of this model. This research finds application in design and processing of novel bulk materials and could lead to processing of bulk nanocomposite materials with tailored properties.

**Contribution to the Army's mission and benefit to society**

The ability to create user-specified, organized patterns of nanoparticles in a macroscale volume of polymer material is anticipated to expedite the future bulk processing of polymer-based multi-functional nanocomposite materials with tailored properties. Nanocomposite materials attempt to take advantage of the unique physical and mechanical properties of nanoparticles (e.g. carbon nanotubes) to create ultra-high strength-to-weight and stiffness-to-weight ratio materials with mechanical properties that outperform those of state-of-the-art materials, at a fraction of the cost. These materials could be used to replace traditional materials such as metals, to reduce strain on the Warfighter by reducing payload. Lightweight materials could furthermore improve energy efficiency of rolling stock, to sustain dominance in military operations over land. In addition, society could benefit from these strong, lightweight materials in the context of energy efficiency of vehicles, amongst other civilian applications. In addition, the ability to tailor patterns of nanoparticles embedded in a polymer matrix by means of ultrasound directed self-assembly, opens the door to designing and manufacturing multi-functional materials with tailored properties, beyond improving mechanical properties and manufacturing lightweight materials.

## 1. Statement of the problem studied

The **scientific objective** of this research is to understand how ultrasound waves can be used to create large-scale, user-specified patterns of nanoparticles dispersed in a host medium. The overarching **engineering objective**, to which this research applies, is to manufacture macroscale polymer-based, multi-functional nanocomposite materials with tailored properties.

We have formulated the following two research tasks.

**Task 1:** Derive the theory and implement a model to simulate organizing nanoparticles into user-defined orientations and patterns in a host medium using ultrasound directed self-assembly (DSA).
**Anticipated result and deliverable:** A scientific tool to predict particle organization, pattern, and orientation, based on the operating and design parameters of the ultrasound transducers, and the properties of the particles and host medium material.
**Task 2:** Experimentally demonstrate that user-specified patterns and orientations of nanoparticles dispersed in a host medium can be obtained using ultrasound directed self-assembly.
**Anticipated result and deliverable:** Validation of the theory and model developed in Task 1.

## 2. Summary of most important results

During the 9 month STIR contract, we have achieved the following key results:

- We have derived the theory and implemented a model to simulate the physics of two-dimensional ultrasound directed self-assembly.
- We have packaged the ultrasound directed self-assembly model into a scientific tool with user-friendly graphical user interface (GUI). The GUI allows the user to solve any ultrasound directed self-assembly problem in two dimensions, without having to understand the underlying model.
- We have experimentally validated our ultrasound directed self-assembly model in water and polymer.

In the remainder of Section 2, we will discuss each of the key results in greater detail.

### 2.1 Developing an ultrasound directed self-assembly model

Enabling the practical implementation of ultrasound DSA as a manufacturing technique requires linking the transducer arrangement and settings that generate the standing ultrasound wave field, to the resulting patterns of nanoparticles. This translates into two problems: (1) the **forward problem** entails calculating the pattern of nanoparticles resulting from user-specified transducer settings, and (2) the **inverse problem** involves calculating the transducer settings required to achieve a user-specified pattern. In both cases the transducer arrangement is also user-specified.

The forward problem is solved by computing the acoustic radiation force associated with the standing ultrasound wave field. The resulting pattern of nanoparticles is then calculated as the stable fixed points $\mathbf{x}_f$ of the acoustic radiation force, defined as the location(s) where the force is zero and points toward $\mathbf{x}_f$ in the surrounding region [1]. The inverse problem is solved either directly or indirectly, for specific reservoir geometries, transducer arrangements, and patterns of nanoparticles. For circular reservoirs lined with transducers that are equipped with backing and absorbing layers to remove reflected ultrasound waves, the transducer phases to create dot patterns are calculated directly as a function of the desired geometry [2,3]. Alternatively, the inverse problem is solved indirectly by first solving the forward problem for a range of possible transducer settings to create a "map" of achievable patterns as a function of the transducer settings [4-6]. However, these existing methods fail to provide a general solution to the inverse problem, because a unique function or map must be derived for each specific reservoir geometry, transducer arrangement, or user-specified pattern geometry. Conversely, using ultrasound DSA as a manufacturing technique requires the ability to calculate transducer settings for any feasible user-specified pattern of nanoparticles, using a reservoir with an arbitrary geometry and transducer arrangement. Theoretically, an infinite number of transducers enables assembly of any user-specified pattern. However, fewer transducers limit the patterns that are feasible to assemble with the ultrasound wave field.

Thus, we demonstrate a direct solution methodology to the inverse problem for any feasible user-specified pattern within a 2D reservoir with an arbitrary simply-closed geometry and transducer arrangement. We accomplish this by linking the transducer settings to the obtained patterns in two steps. First we calculate the standing ultrasound wave field in an arbitrary shaped reservoir lined with transducers around its perimeter as a function of the transducer settings, using the boundary element method based on Green's third identity [7], which relates the wave field within a simply-closed domain to the boundary conditions imposed on the perimeter of the domain. Then, we apply Gor'kov's method [1,8] of calculating the acoustic radiation force acting on a

spherical particle to determine the pattern of nanoparticles resulting from the standing ultrasound wave field. The inverse problem is then posed as an optimization problem whose solution is found using eigendecomposition. A theoretical derivation and experimental validation is presented.

Figure 1 shows a 2D reservoir of arbitrary geometry filled with a fluid medium of density $\rho_m$ and sound speed $c_m$, and with $N_t$ transducers of density $\rho_t$ and acoustic impedance $Z_t$ around the perimeter. The inset of Fig. 1 shows a magnified view of a section of the reservoir, illustrating the discretization of the boundary into $N_b$ boundary elements ($N_b \geq N_t$) and the domain into $N_d$ domain points (red dots), which can be selected in any arrangement. The $j^{\text{th}}$ boundary element, identified by its center point $\mathbf{q}_j$ is $\varepsilon(\mathbf{q}_j)$ wide, and is driven by the transducer setting $v(\mathbf{q}_j)$, i.e., the complex harmonic velocity (amplitude and phase) of the transducer surface along the normal direction $\mathbf{n}(\mathbf{q}_j)$. Additionally, a test point $\mathbf{x}_l$ within the reservoir is indicated with respect to the reservoir origin $\mathbf{o}$.

We use the boundary element method to calculate the ultrasound wave field with frequency $\omega_0$ in terms of the time-independent, complex scalar velocity potential $\varphi$, at each domain point within $D$. We note that: (1) $\varphi$ must be a wave and, thus, satisfy the Helmholtz equation ($\nabla^2\varphi + k_0^2\varphi = 0$) in $D$, where $k_0 = \omega_0/c_m$ is the wave number of the ultrasound wave field in the fluid-medium. (2) The impedance boundary condition $\partial\varphi/\partial\mathbf{n} + ik_0\bar{Z}\varphi = (\rho_t/\rho_m)v$ must be satisfied on $S$, where $\bar{Z} = \rho_m c_m/Z_t$ is the impedance ratio, accounting for the absorption and reflection of the ultrasound wave within the fluid-medium as it interacts with the transducers. (3) $\varphi$, $\nabla\varphi$, and $\nabla^2\varphi$ must be continuous in $D$ and on $S$, except where the boundary is non-smooth (e.g. sharp corners of the reservoir), satisfying the assumptions of Green's third identity [7]. By arranging the values of $v$ for each transducer into a vector $\mathbf{v}$ the ultrasound wave field in $D$ is calculated as [9]

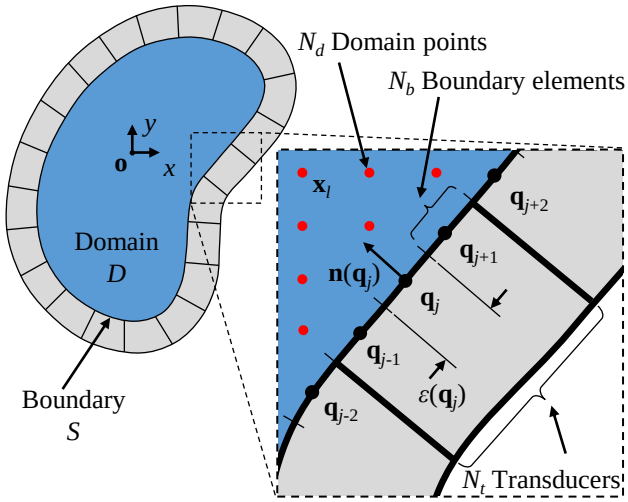


Figure 1: 2D fluid-filled reservoir with arbitrary geometry, lined with $N_t$ transducers. The insert illustrates the discretization scheme used by the boundary element method, dividing the boundary into $N_b$ boundary elements (black dots) and the domain into $N_d$ domain points (red dots). Additionally, the insert shows the length $\varepsilon(\mathbf{q}_j)$ and normal direction $\mathbf{n}(\mathbf{q}_j)$ of the $j^{\text{th}}$ boundary element centered at $\mathbf{q}_j$.

$$\boldsymbol{\varphi} = \mathbf{PWv}\,. \qquad (1)$$

The matrix $\mathbf{W}$ maps each boundary element to its corresponding transducer, i.e., $w_{jm} = 1$ if the $j^{\text{th}}$ boundary element is contained within the $m^{\text{th}}$ transducer, otherwise $w_{jm} = 0$. Additionally, each term $p_{lj}$ of the matrix $\mathbf{P}$ corresponds to the ultrasound wave field created in $\mathbf{x}_l$ by a point source located at $\mathbf{q}_j$ on $S$, including all reflections from the reservoir walls. All $p_{lj}$ terms are calculated in matrix form as

$$\mathbf{P} = \left[\hat{\mathbf{B}} - \hat{\mathbf{A}}\left(\tfrac{1}{2}\mathbf{I} + \mathbf{A}\right)^{-1}\mathbf{B}\right], \qquad (2)$$

for all $N_d$ domain points. Here, $\mathbf{I}$ is the identity matrix and each term $a_{lj}$ and $b_{lj}$ of the matrices $\mathbf{A}$ and $\mathbf{B}$ are calculated as

$$a_{lj} = \left[ ik_0 \bar{Z} G\left(\mathbf{q}_j, \mathbf{x}_l\right) + \frac{\partial G\left(\mathbf{q}_j, \mathbf{x}_l\right)}{\partial \mathbf{n}(\mathbf{q}_j)} \right] \text{, and (3)}$$
$$\times \varepsilon\left(\mathbf{q}_j\right) \delta\left(\mathbf{q}_j, \mathbf{x}_l\right)$$
$$b_{ij} = \frac{\rho_t}{\rho_m} G\left(\mathbf{q}_j, \mathbf{x}_l\right) \varepsilon\left(\mathbf{q}_j\right) \delta\left(\mathbf{q}_j, \mathbf{x}_l\right). \qquad (4)$$

$i = (-1)^{1/2}$ is the unit imaginary number, the function $\delta(\mathbf{q}_j, \mathbf{x}_l) = 0$ when $\mathbf{q}_j = \mathbf{x}_l$, otherwise it is 1, and $G(\mathbf{q}_j,\mathbf{x}_l)$ is the Green's function, which represents the free-field ultrasound wave emitted from a point-source located at $\mathbf{q}_j$ and measured at location $\mathbf{x}_l$ , defined in 2D as

$$G\left(\mathbf{q}_j, \mathbf{x}_l\right) = -\frac{i}{4} H_0\left(k_0 \left|\mathbf{q}_j - \mathbf{x}_l\right|\right). \qquad (5)$$

Here, $H_0$ is the $0^{\text{th}}$ order Hankel function of the first kind, and $|\mathbf{q}_j - \mathbf{x}_l|$ is the Euclidean distance between points $\mathbf{q}_j$ and $\mathbf{x}_l$. The matrices $\hat{\mathbf{A}}$ and $\hat{\mathbf{B}}$ in Eq. (2) are calculated using the same formulas as $\mathbf{A}$ and $\mathbf{B}$, differing only by the selection of the points $\mathbf{x}_l$, which lay on $S$ for $\mathbf{A}$ and $\mathbf{B}$, and lay in $D$ for $\hat{\mathbf{A}}$ and $\hat{\mathbf{B}}$. Thus, using the boundary element method we link the transducer settings to the resulting ultrasound wave field.

To link the ultrasound wave field to the final pattern of nanoparticles, we calculate the acoustic radiation force acting on a nanoparticle of density $\rho_p$ and sound speed $c_p$, dispersed in a fluid medium at location $\mathbf{x}_l$ in $D$, as

$$\mathbf{f}_l = -\nabla U_l, \qquad (6)$$

where $U_l$ is the acoustic radiation potential in $\mathbf{x}_l$. For a spherical particle with radius $r_p \ll \lambda_0$, where $\lambda_0 = 2\pi\omega_0/c_f$, $U_l$ is calculated as [1,8]

$$U_l = \mathbf{v}^H \mathbf{Q}_l \mathbf{v}, \qquad (7)$$

where $\mathbf{v}^H$ is the conjugate transpose of $\mathbf{v}$, and the matrix $\mathbf{Q}_l$ is calculated as

$$\mathbf{Q}_l = 2\pi r_p^3 \rho_m \mathbf{W}^H \left\{ \frac{1}{3} k_0^2 \left[ 1 - \left( \frac{\beta_p}{\beta_m} \right)^2 \right] \left[ \mathbf{p}_l \mathbf{p}_l^H \right] - \left[ \frac{\rho_p - \rho_m}{2\rho_p + \rho_m} \right] \left[ \left(\nabla \mathbf{p}_l\right) \left(\nabla \mathbf{p}_l\right)^H \right] \right\} \mathbf{W} \qquad (8)$$

Here, $\mathbf{p}_l^H$ is the $l^{\text{th}}$ row of $\mathbf{P}$, and $\beta_m = 1/\rho_m c_m$ and $\beta_p = 1/\rho_p c_p$ is the compressibility of the fluid medium and particle, respectively. From Eq. (7), the final pattern of nanoparticles is calculated as the region(s) consisting of points $\mathbf{x}_l$, where $U_l$ is locally minimum. Thus, to achieve a user-defined pattern consisting of the set of desired points $X_{des}$, each value $U_l$, corresponding to each point $\mathbf{x}_l \in X_{des}$, must be locally minimum. To pose this as an optimization problem with a single objective function, we relax the requirement of local minimality. Instead, we aim to minimize the average value of $U_l$ over all points $\mathbf{x}_l \in X_{des}$, which is written as the quadratic function$_s$

$$\hat{U} = \mathbf{v}^H \hat{\mathbf{Q}} \mathbf{v}, \qquad (9)$$

where the matrix $\hat{\mathbf{Q}}$ is the average of the matrices $\mathbf{Q}_l$ corresponding to each desired point $\mathbf{x}_l \in X_{des}$. The matrix $\hat{\mathbf{Q}}$ is indefinite because $\hat{U}$ has no lower bound. Physically, this occurs because particles can be trapped at the desired positions more effectively by increasing the amplitudes of the transducers indefinitely ($|\mathbf{v}| \to \infty$). Practically, the function generator used to excite the transducers limits the transducer amplitudes to finite values and, thus, we constrain the magnitude $|\mathbf{v}| = \alpha$, where $\alpha$ is a real, scalar value representing the maximum harmonic velocity that can be achieved

with a function generator and transducer. Hence, we formulate the constrained quadratic optimization problem

$$\min \hat{U} \text{ , subject to } |\mathbf{v}| = \alpha \text{ .} \qquad (10)$$

From Eq. (10), the optimal transducer settings **v*** are calculated as the eigenvector of length $\alpha$ corresponding to the smallest eigenvalue of $\hat{\mathbf{Q}}$. Thus, we solve the inverse problem, finding the transducer settings **v*** required to achieve a feasible user-specified pattern of nanoparticles, defined as a set of desired points $X_{des}$.

### 2.2 Packaging the ultrasound directed self-assembly model as a scientific tool

We have packaged this model in a user-friendly graphical user interface (GUI). The GUI enables solving both the forward and inverse problem, and simulating ultrasound directed self-assembly, without the need to handle the source code of the model. The GUI allows selecting the reservoir dimensions, transducer arrangement and properties, host medium and particle properties. In the case of solving the forward problem, the model calculates the pattern of nanoparticles that is obtained for the selected properties, and for user-specified transducer inputs. Conversely, in the case of solving the inverse problem, the model finds the transducer settings needed to obtain a user-specified pattern of nanoparticles for the selected properties. Figure 2 shows a screenshot of the scientific tool and GUI that we have developed to package the ultrasound DSA model and enable easy access to running simulations. **We have included two movies illustrating the use of the GUI to solve the forward problem (Appendix 1) and the inverse problem (Appendix 2). In addition, we have included a ZIP file with all source code and an executable file that allows running the scientific tool across different platforms (Appendix 3).**

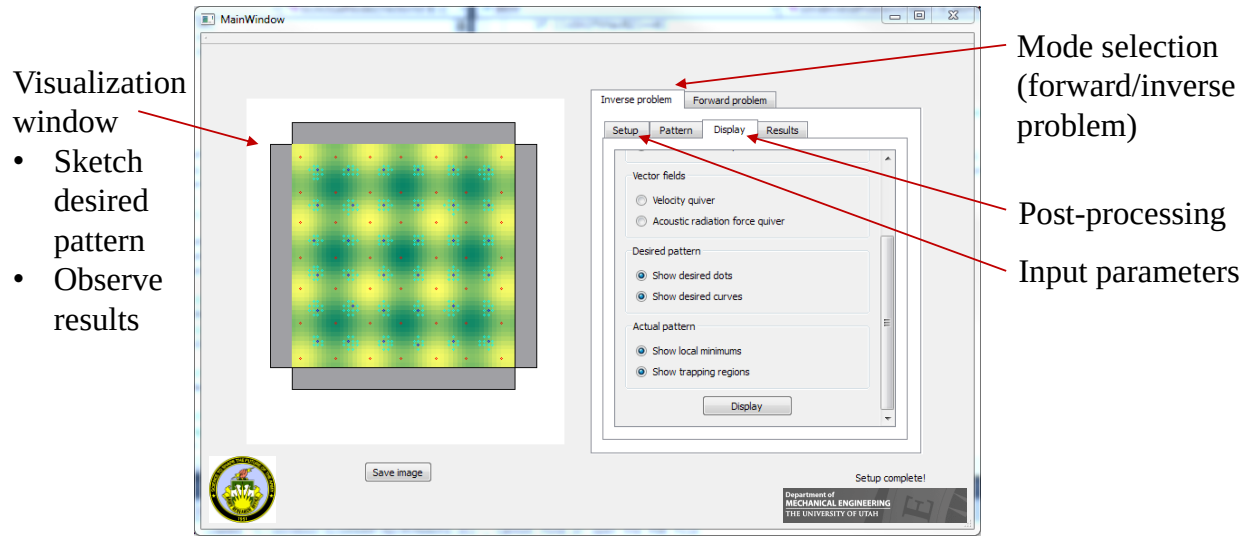


Figure 2: Scientific tool developed to package the ultrasound directed self-assembly model, showing the graphical user interface (GUI) that enables solving the forward and inverse problem, and post-process the results.

### 2.3 Experimental validation in water

Figure 3 shows a schematic of the experimental apparatus that we have used to validate our model. A 12.75×12.75 mm square reservoir containing water with dispersed 80 nm carbon nanoparticles is simulated using our model described in Section 2.1, and manufactured to experimentally validate the model. In both the model and experiment, each of the four reservoir walls consists of a single PZT transducer (type SM112) with center frequency 1.5 MHz, driven by the complex transducer settings (amplitude and phase) $v_1$, $v_2$, $v_3$, and $v_4$, respectively. The optimal transducer settings needed to create a feasible user-specified pattern are computed by solving Eq. (10) and then applied to the transducers in the experimental setup to validate the actual pattern of nanoparticles.

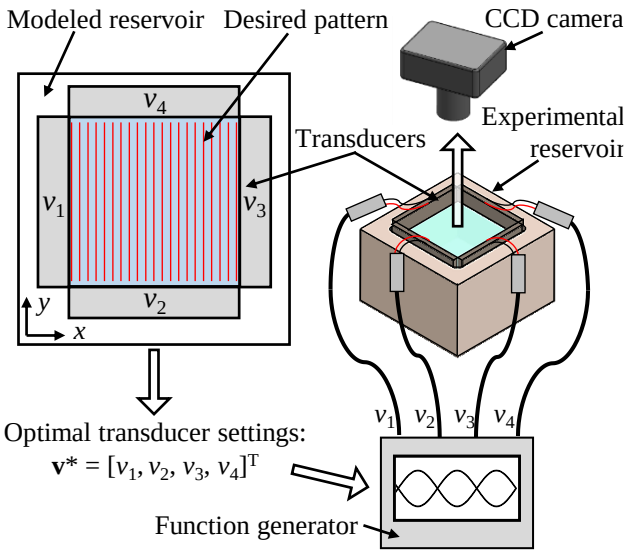


Figure 3: Experimental apparatus. A user-specified pattern is defined within the modeled reservoir, then the inverse problem is solved, yielding the optimal transducer settings which are applied to the machined reservoir, generating the actual pattern of nanoparticles. A CCD camera is then used to image the actual pattern.

Figure 4 shows the two types of patterns that can be achieved in a square reservoir with one transducer per side. These patterns consist either of (a) lines spaced $\lambda_0/2$ apart, oriented along either the *x*- or *y*-directions, or (b) dots arranged in a square grid formation spaced $\lambda_0/2$ apart in both the *x*- and *y*-directions. The user-defined pattern is depicted in red, from which the complex transducer setting (amplitude and phase) are calculated using the "inverse" method explained in section 2.1 of this report. These settings are then applied to the respective transducers, and the 80 nm carbon nanoparticles assemble into the user-specified pattern. A picture of the experimentally obtained pattern is shown, and an inset shows a magnified view of the experimental results, overlaid with the user-specified pattern. The line and dot patterns can also be shifted in the *x*- or *y*-direction. To validate our method of solving the inverse problem in an unconstrained fashion, we have prescribed line and dot patterns at positions shifted along the *x*- and *y*- direction over a distance of $\Delta x \in [0, \lambda_0/2)$, demonstrating that user-specified patterns can be created throughout the reservoir. For each pattern we compare the user-specified pattern to the experimentally obtained pattern by calculating the pattern error

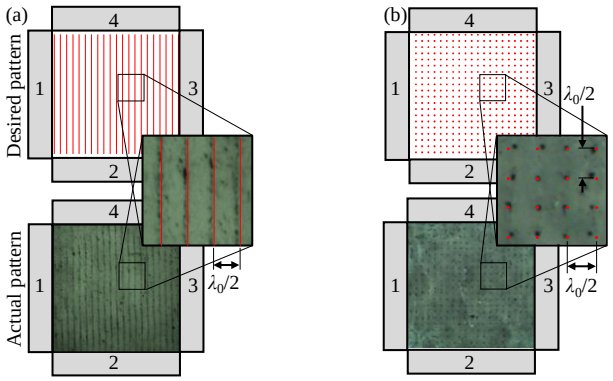


| Transducer | Amplitude [m/s] | Phase [deg.] |
|---|---|---|
| 1 | 0.70 | -141.34 |
| 2 | 0.00 | 0.00 |
| 3 | 0.71 | -142.96 |
| 4 | 0.00 | 0.00 |

| Transducer | Amplitude [m/s] | Phase [deg.] |
|---|---|---|
| 1 | 0.50 | 180.00 |
| 2 | 0.50 | -2.29 |
| 3 | 0.50 | 177.70 |
| 4 | 0.50 | 0.00 |

Figure 4: Experimental results indicating the desired patterns (red) and actual patterns (black) created using the optimal transducer settings calculated using Eq. (9) for a desired (a) line pattern and (b) dot pattern of nanoparticles.

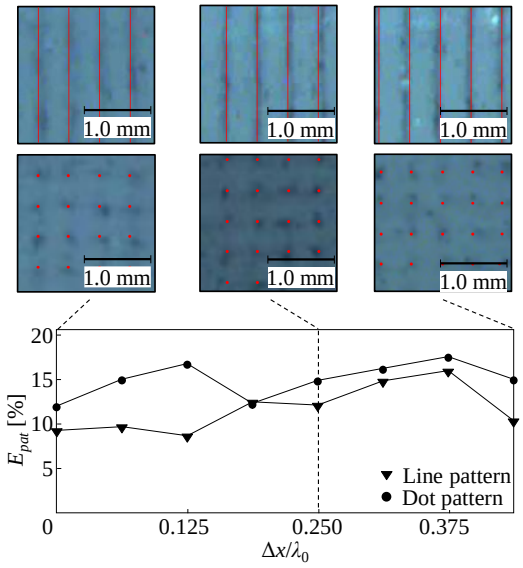


Dot patterns

| Transducer | Setting \ $\Delta x/\lambda_0$ | 0 | 0.063 | 0.125 | 0.188 | 0.25 | 0.313 | 0.375 | 0.438 |
|---|---|---|---|---|---|---|---|---|---|
| 1 | Amplitude [m/s] | 0.69 | 0.69 | 0.58 | 0.40 | 0.15 | 0.14 | 0.40 | 0.59 |
| | Phase [deg.] | 180.00 | 0.00 | 0.00 | 180.00 | 180.00 | 180.00 | 0.00 | -180.00 |
| 2 | Amplitude [m/s] | 0.14 | 0.15 | 0.40 | 0.58 | 0.69 | 0.69 | 0.59 | 0.40 |
| | Phase [deg.] | -163.13 | 164.64 | 177.21 | 2.65 | 15.36 | 163.13 | -2.83 | -177.17 |
| 3 | Amplitude [m/s] | 0.14 | 0.15 | 0.40 | 0.58 | 0.69 | 0.69 | 0.59 | 0.40 |
| | Phase [deg.] | 16.87 | -15.36 | -2.79 | -177.35 | -164.64 | -16.87 | 177.17 | 2.83 |
| 4 | Amplitude [m/s] | 0.69 | 0.69 | 0.58 | 0.40 | 0.15 | 0.14 | 0.40 | 0.59 |
| | Phase [deg.] | 0.00 | 180.00 | 180.00 | 0.00 | 0.00 | 0.00 | 180.00 | 0.00 |

Line patterns

| Transducer | Setting \ $\Delta x/\lambda_0$ | 0 | 0.063 | 0.125 | 0.188 | 0.25 | 0.313 | 0.375 | 0.438 |
|---|---|---|---|---|---|---|---|---|---|
| 1 | Amplitude [m/s] | 0.98 | 0.98 | 0.82 | 0.57 | 0.22 | 0.20 | 0.56 | 0.83 |
| | Phase [deg.] | -130.40 | 40.86 | -136.33 | -138.88 | -153.75 | -114.33 | 53.34 | 50.65 |
| 2 | Amplitude [m/s] | 0.00 | 0.00 | 0.00 | 0.00 | 0.00 | 0.00 | 0.00 | 0.00 |
| | Phase [deg.] | 0.00 | -180.00 | 0.00 | 0.00 | 0.00 | -180.00 | 0.00 | 180.00 |
| 3 | Amplitude [m/s] | 0.20 | 0.22 | 0.57 | 0.82 | 0.98 | 0.98 | 0.83 | 0.56 |
| | Phase [deg.] | 65.67 | 26.22 | -138.88 | -136.33 | 49.60 | -129.35 | -126.66 | 2.83 |
| 4 | Amplitude [m/s] | 0.00 | 0.00 | 0.00 | 0.00 | 0.00 | 0.00 | 0.00 | 0.00 |
| | Phase [deg.] | 0.00 | -180.00 | 0.00 | 0.00 | 0.00 | 180.00 | 0.00 | -180.00 |

Figure 5: Pattern error for desired line and dot patterns as they are shifted the *x*- and *y*-directions in increments of $\Delta x/\lambda_0 = 0.0625$. Additionally, images of the desired dot and line patterns are superimposed over the actual dot and line patterns for the shifted distances $\Delta x/\lambda_0 = \{0.125, 0.250, 0.375\}$.

$E_{pat}$ as the average distance between the centers of the user-specified and experimentally obtained pattern features (lines or dots), normalized by the nominal pattern spacing $\lambda_0/2$. Figure 5 shows the pattern error as a function of the normalized pattern shift distance $\Delta x/\lambda_0$ for line (triangle marker) and dot (dot marker) patterns. Additionally, Fig. 5 shows images of the user-specified patterns superimposed on the experimentally obtained patterns, for line and dot patterns that have been shifted by $\Delta x/\lambda_0 = \{0.125, 0.250, 0.375\}$ in the *x*- and *y*- directions. We observe that the pattern error $E_{pat}$ remains less than 16.0% and 17% for line and dot patterns, respectively, indicating good agreement between the user-specified and experimentally obtained patterns. In practice, these

patterns are not identical due to imperfections in the experiment and assumptions in the model. The reservoir is not perfectly square, and the transducers may be slightly misaligned, which affects the standing ultrasound wave field. Additionally, the model neglects viscous and thermal effects, which can produce acoustic streaming and alter the fluid properties, which are not accounted for in the model.

When adding additional transducers to the setup, more exotic patterns can be created. Figure 6 depicts two examples of patterns that are obtained with two independent transducers per side of a square reservoir, i.e., 8 transducers in total. The user-defined pattern is depicted in red, from

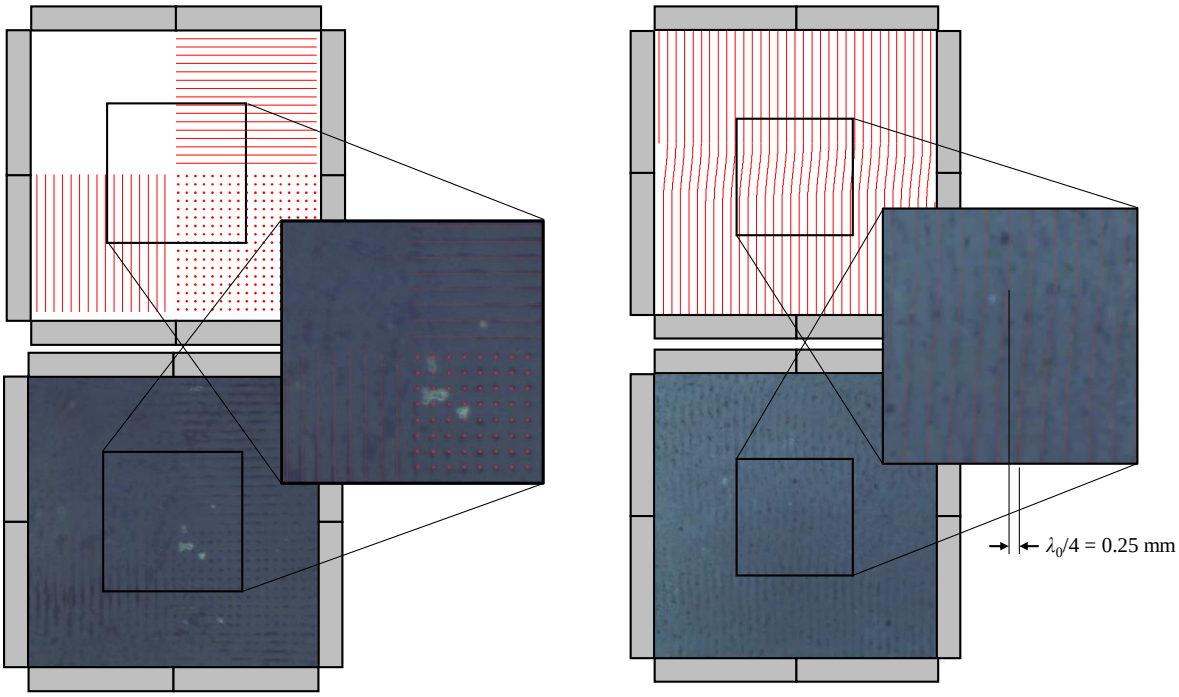


| Transducer | Amplitude [m/s] | Phase [deg.] |
|---|---|---|
| 1 | 0.00 | 180.00 |
| 2 | 0.49 | 32.29 |
| 3 | 0.00 | 0.00 |
| 4 | 0.51 | 32.29 |
| 5 | 0.51 | 32.29 |
| 6 | 0.00 | -180.00 |
| 7 | 0.49 | 32.29 |
| 8 | 0.00 | 0.00 |

| Transducer | Amplitude [m/s] | Phase [deg.] |
|---|---|---|
| 1 | 0.69 | 0.00 |
| 2 | 0.15 | -15.36 |
| 3 | 0.00 | 0.00 |
| 4 | 0.00 | 0.00 |
| 5 | 0.69 | 0.00 |
| 6 | 0.15 | -15.36 |
| 7 | 0.00 | 180.00 |
| 8 | 0.00 | 180.00 |

Figure 6: Exotic patterns obtained with 8 transducers, (a) combined line and dot patterns and (b) a shifted line pattern. Red line depicts user-specified pattern, and picture shows experimental implementation.

which the complex transducer setting (amplitude and phase) are calculated using the "inverse" method explained in section 2.1 of this report. These settings are then applied to the respective transducers, and the 80 nm carbon nanoparticles assemble into the user-specified pattern. A picture of the experimentally obtained pattern is shown, and an inset shows a magnified view of the experimental results, overlaid with the user-specified pattern.

### 2.4 Experimental validation in polymer

We have used ultrasound directed self-assembly to manufacture dogbone specimens of polymer matrix composite materials with aligned carbon nanotubes (CNTs) as reinforcement. We have focused on manufacturing materials with a CNT weight fraction in excess of 1%, as it is well-known that small weight fractions have a limited effect on the mechanical properties of the material. A dogbone shaped reservoir is machined from high density polyethylene, which displays low adhesion to the polymer matrix material and allows easy extraction of the finished composite material specimens from the reservoir. The reservoir is mounted on a removable glass base. Two parallel piezoelectric transducers made of PZT-4, with resonant frequency of 1.5 MHz, are embedded in recess slots cut in the walls of the reservoir, and oppose each other over the entire 18 mm gauge length. The resulting dogbone specimen resembles an ASTM D638 Type V plastic sample, and is sufficiently large (70 mm length) to illustrate that macroscale components can successfully be manufactured using the ultrasound alignment method. Multi-walled carbon nanotubes (MWCNTs) as opposed to single-walled carbon nanotubes (SWCNTs) are used in the experiments because of cost. Figure 7 illustrates the manufacturing and alignment process. MWCNTs with a diameter of 50-80 nm and length of 10-20 μm are added to part A of a two-part, low-viscosity, fast curing thermoset resin (Smooth-Cast 300 thermoset, Smooth-On Inc.) (Fig. 7 a)), and dispersed by means of bath sonication (Fig. 7 b)). Part B of the resin is then added (Fig. 7 c)) prior to transferring the mixture to the dogbone shaped reservoir (Fig. 7 d)). The viscosity of the resin at room temperature is 80 cPs. A standing bulk acoustic wave (BAW) is created between the two opposing PZT plates to align the MWCNTs at the nodes of the standing wave pattern (Fig. 7 e)), when this force exceeds the drag force acting on the MWCNTs. The PZT plates are driven by a function generator (Tektronix, AFG 3102), amplified by a 45 dB 50 W RF power amplifier (Electronic Navigation Industries, 440LA). Cross-linking of the mixture starts immediately following the addition of the second resin part to the mixture. The sample is extracted from the reservoir upon completion of the cross-linking process (Fig. 7 f)).

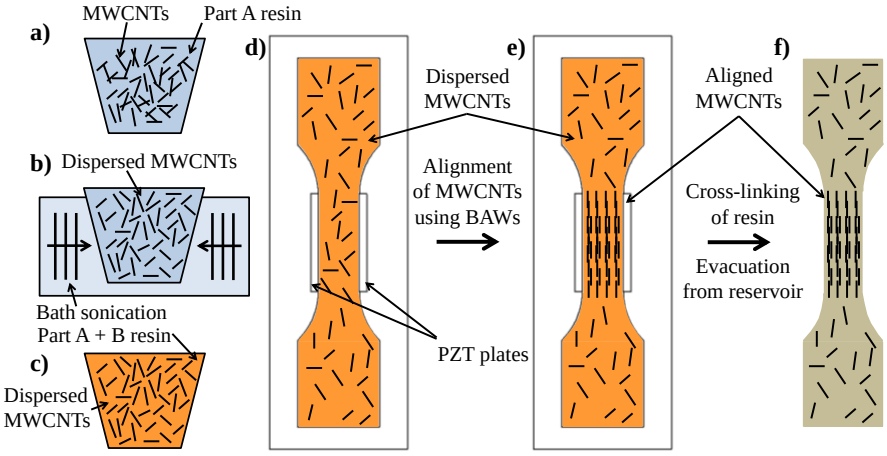


Figure 7: Manufacturing process of a dog-bone shaped composite material specimen with aligned MWCNTs

Figure 8 a) displays a typical example of a dog-bone specimen with one weight percent (wt %) aligned MWCNTs, fabricated using ultrasound waves with a frequency of 1.477 MHz. Figure 8 b)

shows a detail of the gauge section with aligned MWCNTs, obtained with an optical microscope, after locally polishing the surface of the specimen, to reveal the presence of the aligned MWCNTs. The spacing between two rows of aligned MWCNTs is 458 μm, which is expected based on the sound speed of the resin, and the occurrence of two nodes per wave length.

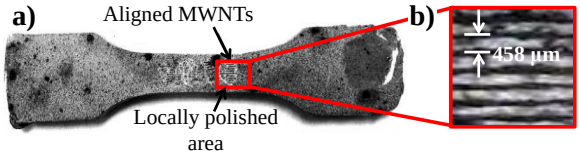


Figure 8: a) Aligning MWCNTs in a 70 mm long dog bone sample, showing the scalability of the acoustic alignment technique to align MWCNTs in a polymer matrix material. This sample contains 5 Vol% (1 wt%) MWCNTs. A small section is polished to reveal the presence of the aligned MWCNTs and b) close-up of aligned MWCNTs

We have performed quasi-static tensile testing for specimens with MWCNT weight fraction between 1 and 10% and compared the Young's modulus and ultimate tensile strength to virgin polymer material, and to polymer material with 1 weight percent randomly oriented MWCNTs. We observed that the ultimate tensile strength and Young's modulus increase with increasing CNT weight fraction, and observed that randomly oriented MWCNTs do not significantly improve the mechanical properties of the polymer matrix material, in line with previous research. However, we obtained a 200% increase in the ultimate tensile strength for the case of 10% weight fraction of MWCNTs aligned in the polymer matrix.

## 3. Conclusion

We have derived a method of ultrasound DSA which, for the first time, provides a direct solution to the inverse problem for a reservoir with arbitrary geometry, calculating the transducer settings necessary to achieve any feasible user-specified pattern of nanoparticles. In contrast to existing methods in the literature, which are unique to each specific reservoir and pattern, this new method provides a general technique for solving the inverse problem in reservoirs with for arbitrary geometries, transducer arrangements, and patterns. Using a square reservoir, feasible line and dot patterns are specified, and our new method is used to calculate the transducer settings necessary to generate the patterns. These transducer settings are applied to an experimental reservoir, generating the actual patterns of nanoparticles, which are then compared to the desired patterns. Good agreement is found between the desired patterns and the actual patterns, demonstrating our new method's ability to effectively calculate the transducer settings necessary to generate user-specified patterns.

## 4. Research products

**Scientific tool:** We have included the scientific tool developed to simulate ultrasound directed self-assembly in Appendix 3. All source code has been included, and an executable file that launches the GUI of the scientific tool.

**Journal publications:** We have focused during the 9 month project on completing the research and implementing the scientific tool. While we already have published one journal publication, we are still in the process of publishing the research results of this project. We have included a list of the different journal publications that we have published or are preparing. We include the ARO funding in the acknowledgments of all these publications.

Corbitt SJ, Petersen SJ, Francoeur M, Raeymaekers B, State-of-the-art fabrication of Mie resonance-based dielectric metamaterials operating at optical frequencies for use in engineering devices: A review; *Journal of Quantitative Spectroscopy and Radiative Transfer*, Vol. 229(4), pp. 547-556 (2015)

Greenhall JJ, Guevara Vazquez F, Raeymaekers B, Ultrasound directed self-assembly of 2D arbitrary patterns of nanoparticles, in preparation for submission (2015)

Greenhall JJ, Guevara Vazquez F, Raeymaekers B, Two-dimensional constrained optimization methods for ultrasound directed self-assembly, in preparation for submission (2015)

Homel LJ, Greenhall JJ, Raeymaekers B, Aligning ultra-high weight fraction carbon nanotubes in a polymer matrix using bulk ultrasound waves, in preparation for submission (2015)

## 5. Interactions with Army Research Labs

**LJ Holmes:** I have visited LJ Holmes's research group (Micro-Compositronics and Rapid Operations Lab) in July 2013 at Aberdeen Proving Grounds (APG), to discuss a possible collaboration. The idea is to integrate the ultrasound directed self-assembly technique with additive manufacturing. LJ is an expert in additive manufacturing and showed me around his laboratory and several other labs at APG, I also gave a seminar at APG during that visit. During the STIR grant, I have kept regular contact with LJ and have solicited his feedback to ensure that our research is in line with the Army mission.

**Steve Taulbee:** Steve Taulbee visited the University of Utah in January 2015 and I briefly met with him to discuss the Army Research on which we are working. Steve invited me to visit APG again, and I have given a seminar at APG in April 2015, in addition to meeting again with LJ Holmes, Ray Brennan, and others, to discuss our research progress in light of Army needs and future directions.

**Raymond Brennan:** I have had several phone conversations about the fit and a possible collaboration with the Energy Coupled to Matter program, with Ray Brennan. We plan to extend the research performed during this STIR contract to use ultrasound directed self-assembly for manufacturing of multi-functional materials, and we will collaborate with Ray on this effort.

## 6. References

[1] M. Barmatz and P. Collas, Acoust. Soc. Am. **77**, 928 (1985).

[2] C.R.P. Courtney, B.W. Drinkwater, C.E.M. Demore, S. Cochran, A. Grinenko, and P.D. Wilcox, Appl. Phys. Lett. **102**, 123508 (2013).

[3] C.R.P. Courtney, C.E.M. Demore, H. Wu, A. Grinenko, P.D. Wilcox, S. Cochran, and B.W. Drinkwater, Appl. Phys. Lett. **104**, 154103 (2014).

[4] J. Greenhall, F. Guevara Vasquez, and B. Raeymaekers, Appl. Phys. Lett. **103**, 074103 (2013).

[5] T. Kozuka, K. Yasui, T. Tuziuti, A. Towata, and Y. Iida, Japanese J. Appl. Physics, Part 1 Regul. Pap. Short Notes Rev. Pap. **46**, 4948 (2007).

[6] A. Grinenko, C.K. Ong, C.R.P. Courtney, P.D. Wilcox, and B.W. Drinkwater, Appl. Phys. Lett. **101**, 233501 (2012).

[7] L.C. Wrobel, *The Boundary Element Method, Applications in Thermo-Fluids and Acoustics* (John Wiley & Sons, 2002).

[8] L.P. Gor'kov, Sov. Phys. Dokl. **6**, 773 (1962).

[9] N. Vlahopoulos and S.T. Raveendra, J. Sound Vib. **210**, 137 (1998).

## Appendices

We have provided Dropbox links to each of the appendices, as the ARO reporting website does not allow for submitting these extra files. However, we believe they are an intricate part of our reporting.

Appendix 1: Movie demonstrating solving the forward problem with the scientific tool/GUI

https://www.dropbox.com/s/rar5h441umjdzgx/Appendix1.avi?dl=0

Appendix 2: Movie demonstrating solving the inverse problem with the scientific tool/GUI

https://www.dropbox.com/s/9qxvbu18naj6tpr/Appendix2.avi?dl=0

Appendix 3: Source code and cross-platform executable of the scientific tool/GUI

https://www.dropbox.com/s/qwy5c1zooyxthu5/Appendix3.zip?dl=0